Preprint Title	Siloxane Bridge Linked Gold Nanoparticle-Liquid Crystalline Nanocomposite
Authors	Olusegun Amos and Georg H. Mehl
Publication Date	05 Juni 2024
Article Type	Full Research Paper
Supporting Information File 1	TEMPL_ ESI Siloxane Bridge Linked Gold Nanoparticle.docx; 528.0 KB
ORCID® iDs	Olusegun Amos - https://orcid.org/0000-0003-3139-3057

Siloxane Bridge Linked Gold Nanoparticle-Liquid Crystalline Nanocomposite

Olusegun Amos[1,2]*; Georg H. Mehl[1]

[1]Chemistry Department, University of Hull, Hull HU6 7RX, United Kingdom.
[2]Department of Industrial Chemistry, Federal University, Lokoja, P.M.B 1154, Lokoja, Nigeria.
Email: Olusegunamos@yahoo.com; olusegun.amos@fulokoja.edu.ng,
* Corresponding author

Abstract

Gold nanoparticles (AuNPs) composite with the gold surface linked directly with the mesogen through in-situ generated siloxane has been synthesised and is hereby presented. Silane conjunction approach was carried out by capping AuNPs with 11-Marcapto-1-Undecanol (AuNPMUD) while the laterally terminal alkene of the mesogen (1) was converted to triethoxysilane end group (2) by hydrosilylation reaction. The hydrolysis and condensation of the ethoxy group of the mesogen (2) with the hydroxyl group of the capped AuNPs afforded the nanocomposite (3). The nanocomposite showed smectic arrangement under polarised optical microscope.

Keywords

Gold nanoparticles; hydrosilylation; mesogen; nematic; nanocomposites.

Introduction

Due to the self-assembly of AuNPs and the anisotropic characteristic of liquid crystal materials, coupling them together produce new materials with interesting and unique properties [1,2]. These properties have prompted their application in biology/medicine [3,4], catalysis [5], electronic [6,7], chemistry, material science and engineering, and are generally based on their magnetic, electronic and optical behaviour.

When coated with the suitable material, AuNP composites can exhibit 2-D or 3-D arrangements making them processable and self-assembled [8]. Different strategies have been used to induce mesogenic properties into the target molecule such as direct capping of the AuNPs with the mesogens, ligand exchange between alkane thiol capped-AuNPs [9,10] and the mesogens, alkyne/azide click [11].

The silane conjunction approach was described in which mercapto undecanol capped gold nanorods was functionalised with alkoxysilane mesogen [12,13].

Here, we describe the introduction of the ethoxysilane-end mesogen (**2**) with short lateral ethoxysilane end chain (n = 5) unto 11- mercapto-1-undeecanol capped AuNPs (**AuNPMUD**) in which the ethoxy group enable the silane to anchor to the AuNPs via the hydroxyl group thereby forming the siloxane bridge [14] (Figure 1).

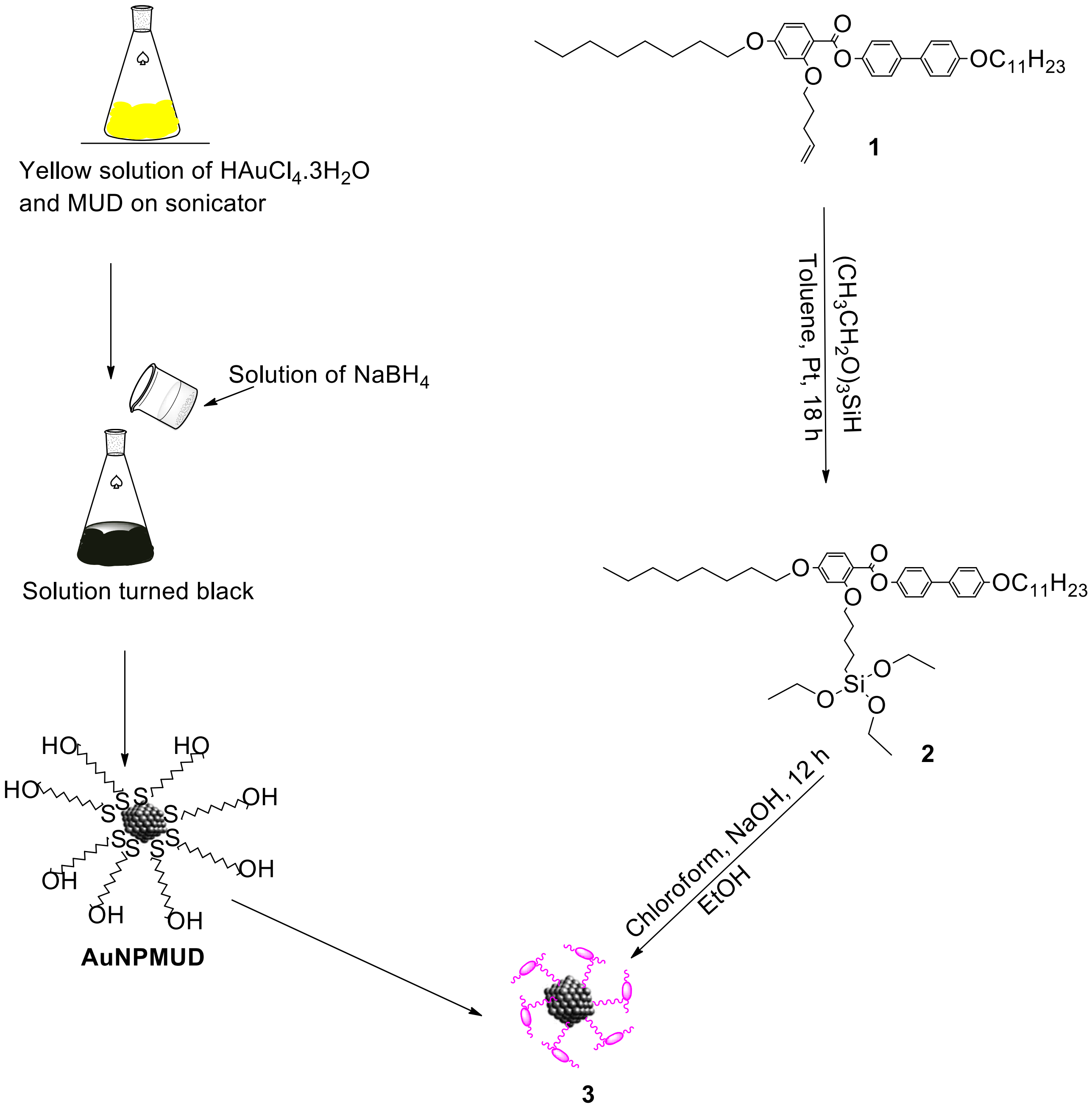

Figure 1: Synthesis of nanocomposite 3.

11-mercapto-1-undecanol-capped AuNPs (~3 nm) was synthesis by modify methods describe in the literature [15,16]. The –OH group of the capped AuNPs provide a linkage point for anchoring the silane.

The mesogen **1** with laterally attached alkene end was synthesized according literature [17] and the alkene end was converted to triethoxysilane group by hydrosilylation [12,13] to form mesogen **2**. The hydrolysis and condensation reactions of the triethoxysilane with the –OH end of the capped AuNPs afforded the target composite **3.**

Results and Discussion

The AuNPs was successfully capped with MUD and was monodispersed as confirmed by TEM Figure **2**, with average size distribution of 3.5 ± 0.38 nm.

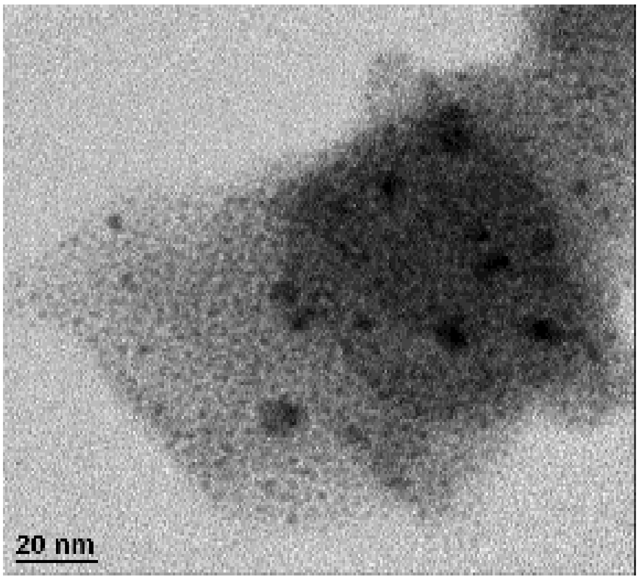

Figure 2: TEM image of AuNPMUD.

The composition elemental analysis (C, H, S) of the MUD-capped AuNPs shows that it is made up of 9.96% C, 1.61 % H and 2.37 % S making a total of 13.94 %. This value is in close agreement with the mass loss from TGA analysis in which one step mass loss of 16.21 % was obtained (Figure **3**). The UV-vis spectrum of AuNPMUD shows absorbance at about 545 nm (Figure **4**).

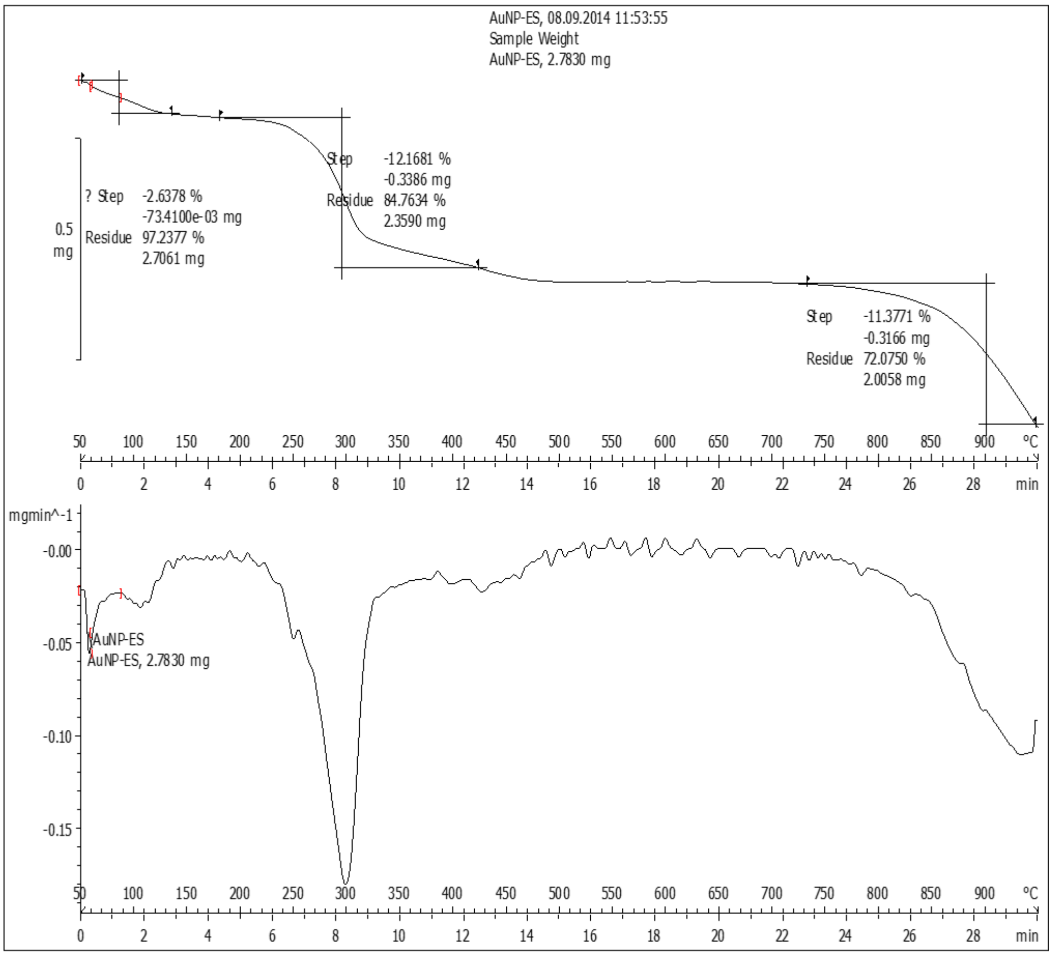

Figure 3: TGA monogram of AuNPMUD.

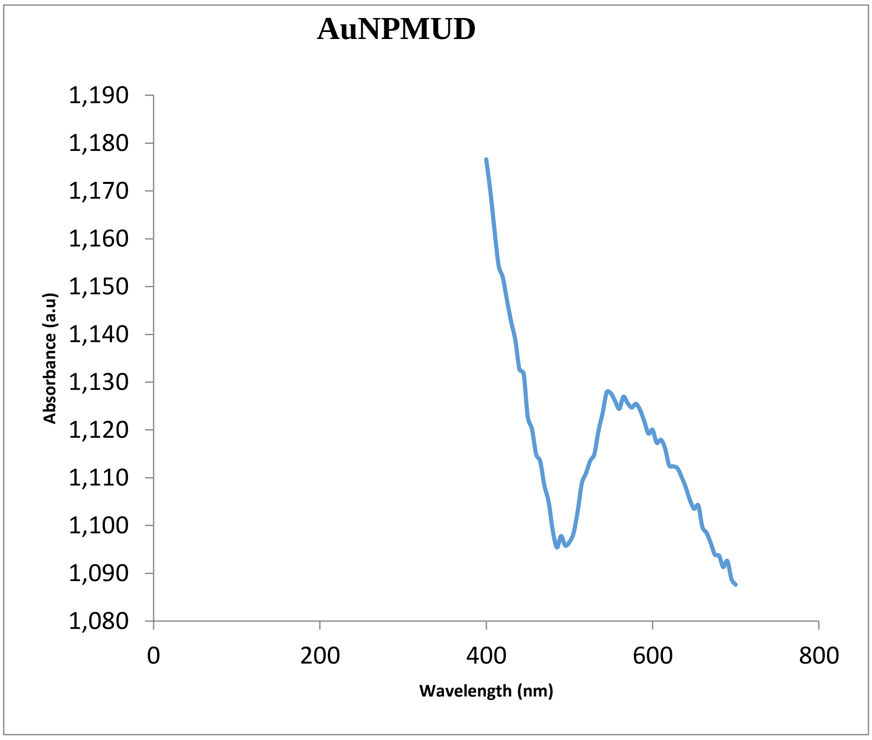

Figure 4. UV-vis of AuNPMUD.

The composite **3** formed after the reaction of AuNPMUD with **2**, was monodispersed as confirmed by TEM (Figure **5**), with average size of 3.59 ± 0.4 nm. The optical texture observed by POM (Figure **6**) shows birefringence characteristics of composites with high metal content. The thermal behaviour of composite **3** when investigated on DSC (Figure **7**) shows a broad peak between 55 ^{o}C and 110 ^{o}C which is also peculiar to metal nanocomposite of this nature.

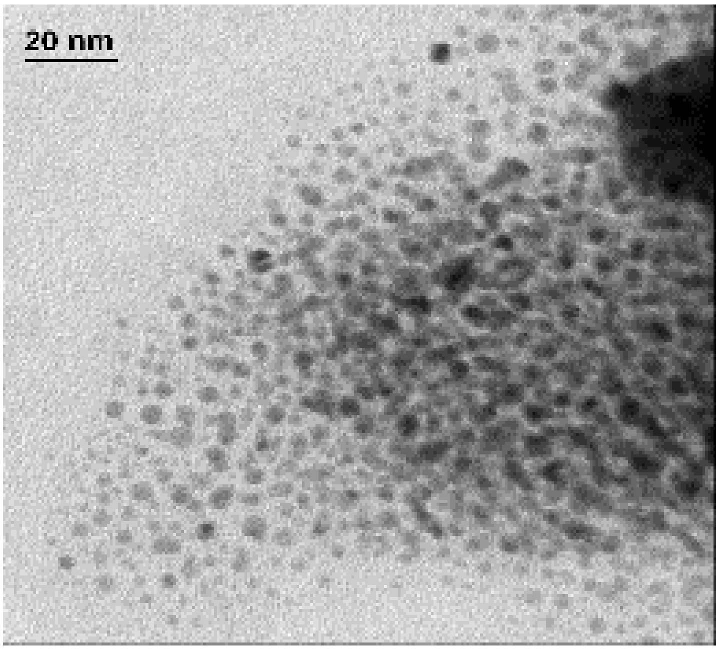

Figure **5:** TEM image of Composite **3**.

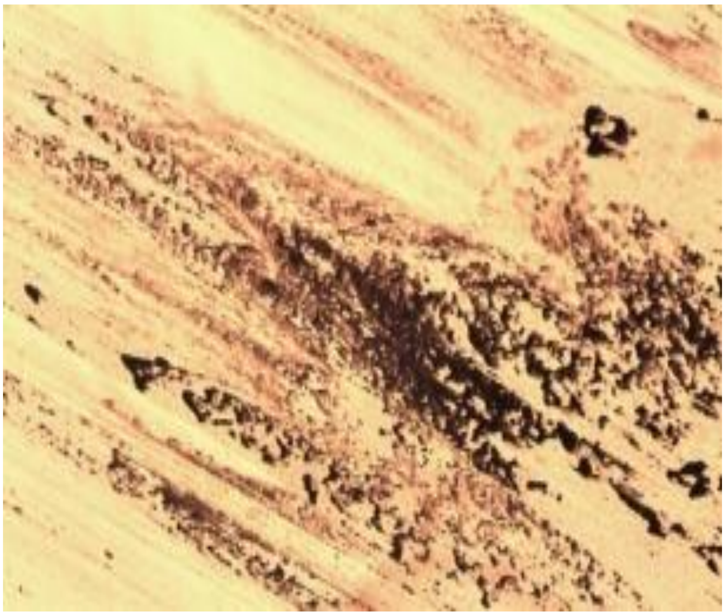

Figure 6: POM of Composite **3**.

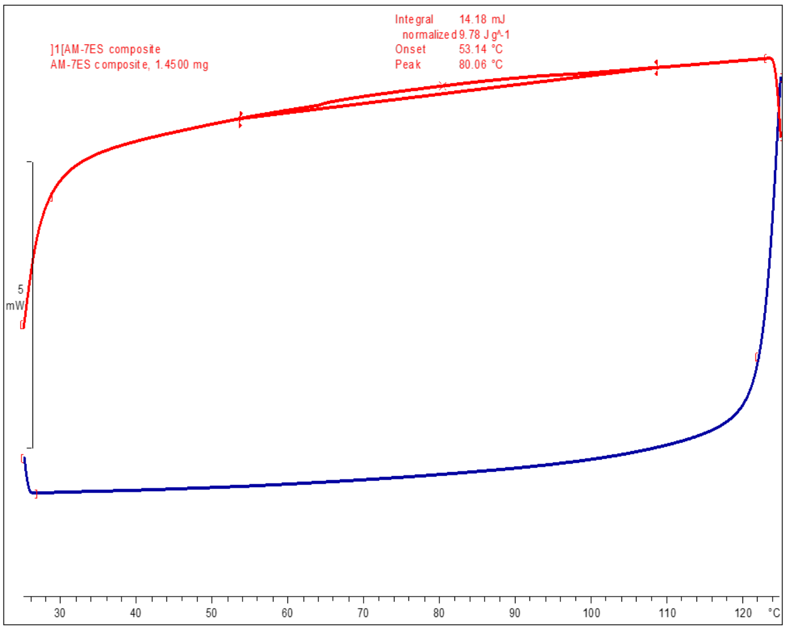

Figure 7: DSC curves of Composite **3**.

Thermogravimetry analysis (TGA) of the composite **3** (Figure **8**) shows two step mass losses, the first loss of 5.47 % between 50 - 110 ºC is attributed to water loss/condensation by-products of organic alkoxy silane compounds, and the second loss of 14.67 % between 110 – 410 ºC is attributed to loss of ligands.

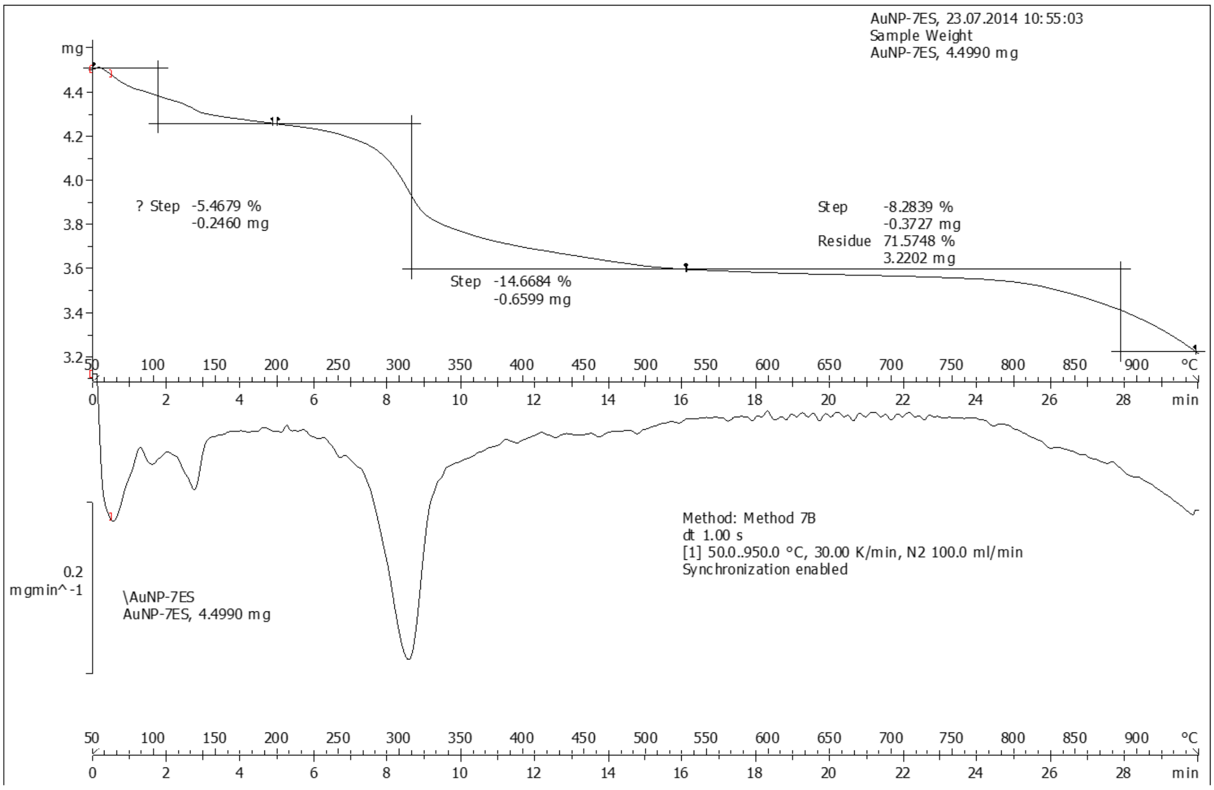

Figure 8: TGA of Composite **3**.

The total mass loss (organic content) for the composite is 14.81 % while the residue is 85.19 % which account for gold content. The composition elemental analysis (C, H, S) of **3** shows that it made up of 12.67 % C, 1.91 % H and 1.95 % S, making total of 16.53 %. This value is in close agreement with that obtained from TGA above. The UV-vis spectrum of **3** shows a plasmonic peak at about 540 nm (Figure **9**).

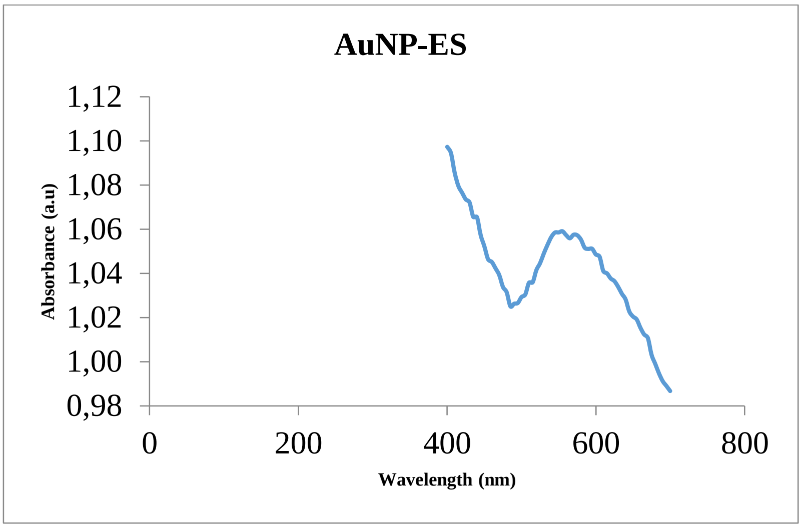

Figure 9: UV-vis of Composite **3**.

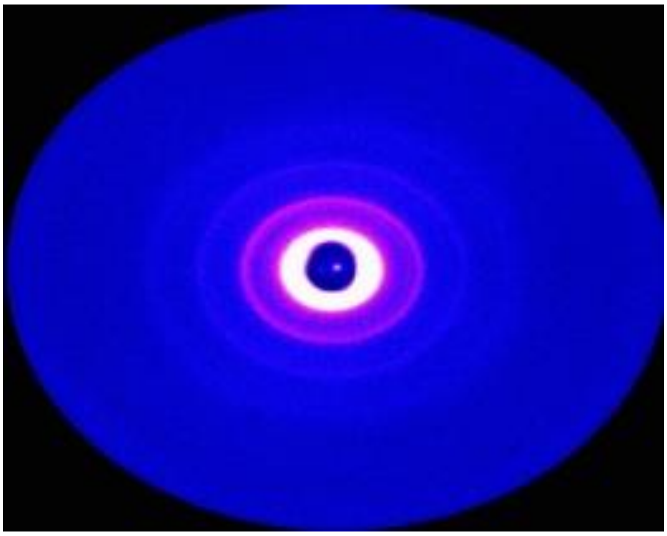

Figure 10: XRD of Composite **3**.

The result of XRD for composite **3** shows reflection angles at 2θ = 2.49 ° (d = 35.5 Å), 5.0 ° (d = 17.7 Å), and 7.6 ° (d = 11.8 Å) (Figure **10**) which corresponds to (001), (002) and (003) reflections fitting to a smectic layering of 35.5 Å. This is the first example of such a laterally allocated mesogen not showing columnar but smectic organisation of the gold nanoparticles in layers. The size of the AuNP can be estimated from the strong (001) Bragg reflection in the XRD at $2\theta = 2.49\ ^{o}$ in which it is 35.5 Å (3.55 nm), which is in very good agreement with the TEM value (3.589 nm).

From the XRD, TEM and TGA data, the average number of gold atoms (N_{Au}), the number of ligands per nanoparticles (N_L) and the average molecular weight of the composites (M_W) were estimated [18,19] to be 1437 atoms, 49 atoms and 332628 g/mol respectively.

Conclusion

We have synthesized a novel nanocomposite with siloxane bridge linking the mesogen to the AuNPs and which shows smectic arrangement rather than columnar with 1437 atoms of gold and 49 ligand atoms.

Electronic Supplementary Information (ESI) available: experimental procedures for the synthesis of materials and characterization data are available.

Acknowledgement

This work is based on the doctoral dissertation of the first author Dr. Olusegun Amos, “Synthesis and characterization of gold nanoparticle composites with side chain liquid crystals”, (2015, University of Hull).

References

1. N. Kanayama, N.; Tsutsumi, O.; Kanazawa, A.; Ikeda, T. *Chem. Commun*., 2001, 2640–2641.
2. Qi, H.; Hegmann, T. *Liquid Crystal Today,* 2011*,* **20**, 102-104.
3. Kennedy, L.; Bickford, L.; Lewinski, N.; Coughlin, A.; Hu, Y.; Day, E.; West, J.; Drezek, R. *Small, 2011,***7**, 169-183.
4. Daniel, M. C.; Astruc, D. *Chem. Rev*. 2004, 104, 293−346.
5. Schlêgl, S.; Abd Hamid, S. B. *Angew. Chem. Int. Ed*., 2004,43,1628-1637.
6. Haase, M.; Schäfer, H. *Angew. Chem. Int. Ed*., 2011, 50, 5808–5829.
7. Talapin, D. V.; Lee, J. S.; Kovalenko, M. V.; Shevchenko, E. V. *Chem. Rev*. 2010, 110, 389– 458.
8. Nealon, G. L.; Greget, R.; Dominguez, C.; Nagy, Z. T.; Guillon, D.; Gallani, J. L.; Donnio, B. *Beilstein J. Org. Chem*. 2012, **8**, 349-370.
9. Cseh, L.; Mehl, G. H. *J. Mater. Chem., 2007,* **17***,* 311-315.
10. Cseh, L.; Mehl, G. H. *J. Am. Chem. Soc., 2006,* ***128****, 13376-13377.*
11. Mischler, S.; Guerra, S.; Deschenaux, R. *Chem. Commun*., 2012, **48**, 2183-2185.
12. Umadevi, S.; Feng, X.; Hegmann, T. *Adv. Funct. Mater*., 2013, **23**, 1393–1403.
13. Umadevi, S.; Feng, X.; Hegmann, T. *Ferroelectrics*, 2013, **431**, 164–175.
14. Salon, M. C. B.; Abdelmouleh, M.; Boufi, S.; Belgacem, M. N.; Gandini, A. *J. Coll and interf Sc*, 2005, **289**, 249-261.
15. Raula, J.; Shan, J.; Nuopponen, M.; Niskanen, A.; Jiang, H.; Kauppinen, E. I.; Tenhu, H. *Langmuir*, 2003, **19**, 3499-3504.

16. Di Pasqua, A. J.; Mishler II, R. E.; Ship, Y. L.; Dabrowiak, J. C.; Asefa, T. *Mat Letts*, 2009, **63**, 1876–1879.
17. Zeng, B.; Liu, F.; Fowler, A. G.; Ungar, G.; Cseh, L.; Mehl, G. H.; Macdonald, J. E. *Adv. Mater.*, 2009, **21**, 1746-1750.
18. Kamata, K.; Lu, Y.; Xia, Y. *J. Am. Chem. Soc*., 2003, **125**, 2384-2385.
19. X. Liu, X.; Atwater, M.; Wang, J.; Huo, Q. Colloids and Surfaces B: *Biointerfaces*, 2007, **58**, 3–7.